

Radiation torque on a spherical birefringent particle in the long wave length limit: analytical calculation

Nian Ji, Mengkun Liu, Jihao Zhou, and Zhifang Lin

Surface Physics Laboratory, Department of Physics, Fudan University, Shanghai, China
phlin@fudan.edu.cn

S. T. Chui

Bartol Research Institute, University of Delaware, Newark, Delaware 19716

Abstract: We present an analytical calculation of the radiation torque on a spherical birefringent particle illuminated by plane electromagnetic wave of arbitrary polarization mode and direction of propagation in the small particle limit. The calculation is based on the extended Mie theory and the Maxwell stress tensor formalism. It is found that, even in the small particle limit, the torque is not always normal to the external electric field for the linearly polarized light. For different incident directions and polarization modes of the incident light, the radiation torque τ may exhibit different types of power law dependence on the particle radius a , $\tau \sim a^\gamma$, with the exponent $\gamma = 3, 5$, and 6 . In the presence of viscous drag, the extraordinary axis of the illuminated particle may be aligned by the optical torque with the incident electric field, the incident magnetic field, or, the incident wave vector, depending on the incident polarization mode and material birefringence of the particle.

© 2005 Optical Society of America

OCIS codes: (290.4020) Mie scattering; (260.1440) Birefringence; (140.7010) Trapping; (290.3770) Long-wave scattering

References and links

1. S. Bayouth, T. A. Nieminen, N. R. Heckenberg, and H. Rubinsztein-Dunlop, "Orientation of biological cells using plane-polarized Gaussian beam optical tweezers," *J. Mod. Opt.* **50**, 1581 (2003).
2. K.D. Bonin, B. Kourmanov, and T.G. Walker, "Light torque nanocontrol, nanomotors and nanorockers," *Opt. Express* **10**, 984 (2002).
3. E. Santamato, A. Sasso, B. Piccirillo, and A. Vella, "Optical angular momentum transfer to transparent isotropic particles using laser beam carrying zero average angular momentum," *Opt. Express* **10**, 871 (2002).
4. Z. Cheng, P.M. Chaikin, and T.G. Mason, "Light streak tracking of optically trapped thin microdisks," *Phys. Rev. Lett.* **89**, 108303 (2002).
5. A. I. Bishop, T. A. Nieminen, N. R. Heckenberg, and H. Rubinsztein-Dunlop, "Optical application and measurement of torque on microparticles of isotropic nonabsorbing material," *Phys. Rev. A* **68**, 033802 (2003).
6. P. Galajda and P. Ormos, "Orientation of flat particles in optical tweezers by linearly polarized light," *Opt. Express* **11**, 446 (2003).
7. M. E. J. Friese, T. A. Nieminen, N. R. Heckenberg, and H. Rubinsztein-Dunlop, "Optical alignment and spinning of laser-trapped microscopic particles," *Nature (London)* **394**, 348 (1998); **395**, 621(E) (1998).
8. E. Higurashi, R. Sawada, and T. Ito, "Optically induced angular alignment of trapped birefringent micro-objects by linearly polarized light," *Phys. Rev. E* **59**, 3676 (1999).
9. T. A. Nieminen, N. R. Heckenberg, and H. Rubinsztein-Dunlop, "Optical measurement of microscopic torques," *J. Mod. Opt.* **48**, 405 (2001)

10. M.E.J. Friese, H. Rubinsztein-Dunlop, J. Gold, P. Hagberg, and D. Hanstorp, "Optically driven micromachine elements," *Appl. Phys. Lett.* **78**, 547 (2001).
11. T.A. Wood, H.F. Gleeson, M.R. Dickinson, and A.J. Wright, "Mechanisms of optical angular momentum transfer to nematic liquid crystalline droplets," *Appl. Phys. Lett.* **84**, 4292 (2004)
12. S. Juodkazis, S. Matsuo, N. Murazawa, I. Hasegawa, and H. Misawa, "High-efficiency optical transfer of torque to a nematic liquid crystal droplet," *Appl. Phys. Lett.* **82**, 4657 (2003).
13. A. La Porta and M. D. Wang, "Optical torque wrench: angular trapping, rotation, and torque detection of quartz microparticles," *Phys. Rev. Lett.* **92**, 190801 (2004).
14. A. I. Bishop, T. A. Nieminen, N. R. Heckenberg, and H. Rubinsztein-Dunlop, "Optical microrheology using rotating laser-trapped particles," *Phys. Rev. Lett.* **92**, 198104 (2004).
15. J.A. Stratton, *Electromagnetic theory* (McGraw-Hill, New York, 1941).
16. C.F. Bohren and D R Huffman, *Absorption and scattering of light by small particles* (John Wiley & Sons, New York, 1983).
17. Y.L. Xu, "Electromagnetic scattering by an aggregate of spheres," *Appl. Opt.* **34**, 4573 (1995);
18. Z.F. Lin and S.T. Chui, "Electromagnetic scattering by optically anisotropic magnetic particle," *Phys. Rev. E* **69**, 056614 (2004).
19. J.D. Jackson, *Classical electrodynamics*, 3rd edition (Wiley, New York, 1999).
20. J. Schwinger, L.L. DeRead, K.A. Milton and W-y Tsai, *Classical electrodynamics* (Perseus Books, Reading, 1998).
21. S. Chang and S.S. Lee, "Optical torque exerted on a homogeneous spherelevitated in the circularly polarized fundamental-mode laser beam," *J. Opt. Soc. Am. B* **2**, 1853 (1985).
22. J.P. Barton, D.R. Alexander and S.A. Schaub, "Theoretical determination of net radiation force and torque for a spherical particle illuminated by a focused laser beam," *J. Appl. Phys.* **66**, 4594 (1989).
23. Ø. Farsund and B.U. Felderhof, "Force, torque, and absorbed energy for a body of arbitrary shape and constitution in an electromagnetic radiation field," *Physica A* **227**, 108 (1996).
24. J.H. Crichton and P.L. Marston, "The measurable distinction between the spin and orbital angular momenta of electromagnetic radiation," *Electronic J of Differential Equations* **04**, 37 (2000).
25. M.J. Weber, *Handbook of optical materials* (CRC Press, New York, 2002).

1. Introduction

Recently, much experimental study has been devoted to the radiation torque due to electromagnetic waves on particles that are either geometrically or optically anisotropic [1, 2, 3, 4, 5, 6, 7, 8, 9, 10, 11, 12, 13, 14]. These studies have lead to a wide variety of applications, including the possibility of making measurement of the viscosity on a microscopic scale, changing the orientation of micro-size particles and biological structure, and developing optically driven and controlled micromachines. Compared with experimental study, less attention has been paid to the theoretical understanding of the optical torque on a birefringent (optically anisotropic) particle. In the long wave length limit, La Porta and Wang proposed for linearly polarized light that the radiation torque is given by [13]

$$\boldsymbol{\tau} = \hat{\mathbf{q}}(\chi_o - \chi_e)\tau_0 \sin 2\phi_e \quad (1)$$

where ϕ_e is the angle between the extraordinary axis (EA) of the birefringent particle and the incident electric field \mathbf{E}_{inc} , $\hat{\mathbf{q}}$ is a unit vector normal to \mathbf{E}_{inc} and the polarization induced on the scatterer, and $(\chi_o - \chi_e)\tau_0$ is the maximum magnitude of the optical torque that can be exerted on the particle, with χ_o and χ_e denoting the electrical susceptibilities in the ordinary and the extraordinary directions, respectively. Equation (1) indicates that the torque is proportional to the difference of the electrical susceptibilities $(\chi_o - \chi_e)$ in magnitude, and it is always perpendicular to the external field in direction. However, Eq. (1) does not give the explicit expression of τ_0 . In particular, it is not applicable to some polarization modes of the incident light such as circular polarization.

The purpose of this paper is to present an analytical calculation of the radiation torque on a spherical birefringent particle illuminated by a plane electromagnetic wave of arbitrary polarization mode and direction of propagation in the small particle limit. The calculation is based on the extended Mie theory and the Maxwell stress tensor formalism. It is found that, even in

the small particle limit, the optical torque is not always normal to the external electric field for the linearly polarized incident mode, presenting a striking contrast to Eq. (1). In addition, the torque may be proportional $(\chi_o - \chi_e)$ or $(\chi_o - \chi_e)^2$ depending on the polarization mode of the incident plane wave. It is also found that the radiation torque τ may show different types of power law dependence on the particle radius a for different directions and polarization modes of illumination. In the presence of viscous drag, the EA of the particle may be aligned by the radiation torque with \mathbf{E}_{inc} , the incident magnetic field \mathbf{H}_{inc} , or the incident wave vector \mathbf{k}_0 , depending on the incident polarization mode as well as material birefringence of the particle.

The rest of the paper is organized as follows. In Section 2, we describe the formulation for the scattering problem of a spherical birefringent particle in the long wave length limit. The calculation of the radiation torque based on the Maxwell stress tensor formalism is presented in Section 3. Finally, a summary is given in Section 4.

2. Scattering formulation in the long wave length limit

For a uniaxial birefringent particle with the electric permittivity tensor $\epsilon_0 \epsilon_r \overleftrightarrow{\epsilon}$ given by

$$\epsilon_r \epsilon_0 \overleftrightarrow{\epsilon} = \epsilon_r \epsilon_0 \begin{pmatrix} 1 & 0 & 0 \\ 0 & 1 & 0 \\ 0 & 0 & 1 + u_a \end{pmatrix}, \quad (2)$$

the electric displacement vector \mathbf{D}_I inside the sourceless and homogeneous particle satisfies the wave equation

$$\nabla \times \nabla \times (\overleftrightarrow{\epsilon}^{-1} \cdot \mathbf{D}_I) - k_s^2 \mathbf{D}_I = 0, \quad (3)$$

with $k_s^2 = \omega^2 \epsilon_r \epsilon_0 \mu_0$ and

$$\overleftrightarrow{\epsilon}^{-1} = \begin{pmatrix} 1 & 0 & 0 \\ 0 & 1 & 0 \\ 0 & 0 & \frac{1}{1+u_a} \end{pmatrix}. \quad (4)$$

Here for simplicity, the particle is assumed to be non-absorptive and non-magnetic. ϵ_0 and μ_0 denote, respectively, the permittivity and permeability of the surrounding medium.

The divergenceless property $\nabla \cdot \mathbf{D}_I = 0$ suggests that \mathbf{D}_I be expanded in terms of the vector spherical wave functions (VSWF's) $\mathbf{M}_{mn}^{(1)}(k, \mathbf{r})$ and $\mathbf{N}_{mn}^{(1)}(k, \mathbf{r})$ [15, 16, 17, 18]

$$\mathbf{D}_I = \sum_{n,m} E_{mn} \left[c_{mn} \mathbf{M}_{mn}^{(1)}(k, \mathbf{r}) + d_{mn} \mathbf{N}_{mn}^{(1)}(k, \mathbf{r}) \right], \quad (5)$$

where the prefactor E_{mn} is given by $E_{mn} = i^n E_0 C_{mn}$, with E_0 characterizing the amplitude of the electric field of the incident light and [17]

$$C_{mn} = \left[\frac{2n+1}{n(n+1)} \frac{(n-m)!}{(n+m)!} \right]^{1/2}. \quad (6)$$

The summation $\sum_{n,m}$ implies that n runs from 1 to $+\infty$ and m from $-n$ to $+n$ for each n . In practical calculations, the expansion is supposed to be uniformly convergent and can be truncated at some $n = n_c$. Since we are interested in the calculation of the radiation torque in the long wave length limit, we set $n_c = 2$ throughout the paper, which guarantees the accuracy for the radiation torque up to η^6 , where $\eta = 2\pi a / \lambda_0$ with λ_0 the incident wavelength. Actually, our numerical results showed that for the typical birefringent particles (such as calcite or quartz, see, e.g., [13]) adopted in most experiments, the calculation of the radiation torque can reach

very good convergence (within a few percent) by simply setting $n_c = 2$ for $\eta < 1$. The value of k in Eq. (5) is determined by Eq. (3). To this end, one has to expand $\overset{\leftrightarrow}{\boldsymbol{\varepsilon}}^{-1} \cdot \mathbf{M}_{mn}^{(1)}$ and $\overset{\leftrightarrow}{\boldsymbol{\varepsilon}}^{-1} \cdot \mathbf{N}_{mn}^{(1)}$ in terms of the VSWF's,

$$\begin{aligned}\overset{\leftrightarrow}{\boldsymbol{\varepsilon}}^{-1} \cdot \mathbf{M}_{mn}^{(1)} &= \sum_{v=0}^2 \sum_{u=-v}^{+v} \left[\tilde{g}_{uv}^{mn} \mathbf{M}_{uv}^{(1)} + \tilde{e}_{uv}^{mn} \mathbf{N}_{uv}^{(1)} + \tilde{f}_{uv}^{mn} \mathbf{L}_{uv}^{(1)} \right], \\ \overset{\leftrightarrow}{\boldsymbol{\varepsilon}}^{-1} \cdot \mathbf{N}_{mn}^{(1)} &= \sum_{v=0}^2 \sum_{u=-v}^{+v} \left[\bar{g}_{uv}^{mn} \mathbf{M}_{uv}^{(1)} + \bar{e}_{uv}^{mn} \mathbf{N}_{uv}^{(1)} + \bar{f}_{uv}^{mn} \mathbf{L}_{uv}^{(1)} \right],\end{aligned}\quad (7)$$

where $\mathbf{L}_{mn}^{(1)}$ are the VSWF's [15, 16, 17]. The expansion coefficients are given by [18]

$$\begin{aligned}\tilde{g}_{uv}^{mn} &= \delta_{nv} \delta_{mu} + \frac{(n^2 + n - m^2) u_a \delta_{nv} \delta_{mu}}{n(n+1)} \\ \tilde{e}_{uv}^{mn} &= \frac{i(n+m) m u_a \delta_{n-1,v} \delta_{mu}}{n(2n+1)} + \frac{i(n-m+1) m u_a \delta_{n+1,v} \delta_{mu}}{(n+1)(2n+1)} \\ \tilde{f}_{uv}^{mn} &= -\frac{i(n+m) m u_a \delta_{n-1,v} \delta_{mu}}{(2n+1)} + \frac{i(n-m+1) m u_a \delta_{n+1,v} \delta_{mu}}{(2n+1)} \\ \bar{g}_{uv}^{mn} &= -\frac{i(n+m)(n+1) m u_a \delta_{n-1,v} \delta_{mu}}{n(n-1)(2n+1)} - \frac{i(n-m+1) n m u_a \delta_{n+1,v} \delta_{mu}}{(n+1)(n+2)(2n+1)} \\ \bar{e}_{uv}^{mn} &= \delta_{nv} \delta_{mu} + \frac{[(2n^2 + 2n + 3)m^2 + (2n^2 + 2n - 3)n(n+1)] u_a \delta_{nv} \delta_{mu}}{n(n+1)(2n-1)(2n+3)} \\ \bar{f}_{uv}^{mn} &= -\frac{(n^2 + n - 3m^2) u_a \delta_{nv} \delta_{mu}}{(2n-1)(2n+3)} + \frac{(n+1)(n+m-1)(n+m) u_a \delta_{n-2,v} \delta_{mu}}{(2n-1)(2n+1)}\end{aligned}\quad (8)$$

$$\quad (9)$$

where δ_{mu} is the Kronecker delta, with $\delta_{mu} = 1$ for $m = u$ and $\delta_{mu} = 0$ for $m \neq u$, and use has been made of $n_c = 2$ so all terms with $n > 2$ or $v > 2$ have been neglected.

Inserting Eq. (5) into Eq. (3), with the use of Eq. (7) and after some algebra, one gets a $2n_d \times 2n_d$ eigensystem governing the value of k in Eq. (5),

$$\begin{aligned}\sum_{v=1}^2 \sum_{u=-v}^{+v} \frac{E_{uv}}{E_{mn}} [\tilde{g}_{mn}^{uv} c_{uv} + \bar{g}_{mn}^{uv} d_{uv}] &= \lambda c_{mn}, \\ \sum_{v=1}^2 \sum_{u=-v}^{+v} \frac{E_{uv}}{E_{mn}} [\tilde{e}_{mn}^{uv} c_{uv} + \bar{e}_{mn}^{uv} d_{uv}] &= \lambda d_{mn}.\end{aligned}\quad (10)$$

where $\lambda = k_s^2/k^2$ and $n_d = n_c(n_c + 2) = 8$.

Let λ_l and $(d_{mn,l}, c_{mn,l})^T$ denote, respectively, the l -th eigenvalues and the corresponding eigenvectors of eigensystem Eq. (10), with l running from 1 to $2n_d = 16$. One can then construct a new set of vector functions \mathbf{V}_l based on the eigenvalues λ_l and eigenvectors $(d_{mn,l}, c_{mn,l})^T$,

$$\mathbf{V}_l = -\frac{i\varepsilon_0 \varepsilon_r}{\lambda_l} \sum_{n=1}^2 \sum_{m=-n}^n E_{mn} [c_{mn,l} \mathbf{M}_{mn}^{(1)}(k_l, \mathbf{r}) + d_{mn,l} \mathbf{N}_{mn}^{(1)}(k_l, \mathbf{r})] \quad (11)$$

with $k_l = k_s/\sqrt{\lambda_l}$. It is straightforward to show that \mathbf{V}_l are divergenceless

$$\nabla \cdot \mathbf{V}_l = 0, \quad (12)$$

and satisfy Eq. (3), the wave equation for \mathbf{D}_l ,

$$\nabla \times \nabla \times (\overset{\leftrightarrow}{\boldsymbol{\varepsilon}}^{-1} \cdot \mathbf{V}_l) - k_s^2 \mathbf{V}_l = 0. \quad (13)$$

The electric displacement \mathbf{D}_I is therefore expanded in terms of \mathbf{V}_I ,

$$\mathbf{D}_I = \sum_{l=1}^{2n_d} \alpha_l \mathbf{V}_l, \quad (14)$$

where the expansion coefficients α_l are to be determined by matching the boundary conditions at the surface of sphere. It follow from Eq. (14) that the electric and magnetic fields \mathbf{E}_I and \mathbf{H}_I inside particle can be written as

$$\begin{aligned} \mathbf{E}_I &= \frac{1}{\epsilon_0 \epsilon_r} \overset{\leftrightarrow}{\epsilon}^{-1} \cdot \mathbf{D}_I = - \sum_{n=1}^2 \sum_{m=-n}^n i E_{mn} \sum_{l=1}^{2n_d} \alpha_l \left[c_{mn,l} \mathbf{M}_{mn}^{(1)}(k_l, \mathbf{r}) + d_{mn,l} \mathbf{N}_{mn}^{(1)}(k_l, \mathbf{r}) + \frac{w_{mn,l}}{\lambda_l} \mathbf{L}_{mn}^{(1)}(k_l, \mathbf{r}) \right] \\ &\quad + \sum_{l=1}^{2n_d} i \alpha_l \left[\frac{w_{00,l}}{\lambda_l} \mathbf{L}_{00}^{(1)}(k_l, \mathbf{r}) \right] \\ \mathbf{H}_I &= \frac{-i}{\omega \mu_0} \nabla \times \mathbf{E}_I = - \frac{1}{\omega \mu_0} \sum_{n=1}^2 \sum_{m=-n}^n E_{mn} \sum_{l=1}^{2n_d} k_l \alpha_l \left[d_{mn,l} \mathbf{M}_{mn}^{(1)}(k_l, \mathbf{r}) + c_{mn,l} \mathbf{N}_{mn}^{(1)}(k_l, \mathbf{r}) \right] \end{aligned} \quad (15)$$

with

$$\begin{aligned} w_{mn,l} &= \sum_{v=1}^2 \sum_{u=-v}^{+v} \frac{E_{uv}}{E_{mn}} [\tilde{f}_{mn}^{uv} d_{uv,l} + \tilde{f}_{mn}^{uv} c_{uv,l}], \\ w_{00,l} &= -\sqrt{\frac{2}{15}} u_a d_{02,l}. \end{aligned}$$

The difference from the isotropic particle lies in the fact that the expansion of \mathbf{E}_I includes \mathbf{L}_{mn} terms since $\nabla \cdot \mathbf{E}_I \neq 0$.

The scattered fields \mathbf{E}_s , \mathbf{H}_s and the incident fields \mathbf{E}_{inc} , \mathbf{H}_{inc} in the isotropic surrounding medium have the same form as in the Mie solution [15, 16]. To be specific, the scattered fields ($\mathbf{E}_s, \mathbf{H}_s$) are given by

$$\begin{aligned} \mathbf{E}_s &= \sum_{n=1}^2 \sum_{m=-n}^n i E_{mn} [a_{mn} \mathbf{N}_{mn}^{(3)}(k_0, \mathbf{r}) + b_{mn} \mathbf{M}_{mn}^{(3)}(k_0, \mathbf{r})] \\ \mathbf{H}_s &= \frac{k_0}{\omega \mu_0} \sum_{n=1}^2 \sum_{m=-n}^n E_{mn} [b_{mn} \mathbf{N}_{mn}^{(3)}(k_0, \mathbf{r}) + a_{mn} \mathbf{M}_{mn}^{(3)}(k_0, \mathbf{r})] \end{aligned} \quad (16)$$

where $k_0^2 = \omega^2 \epsilon_0 \mu_0$ with ϵ_0 and μ_0 being, respectively, the scalar permittivity and permeability of the surrounding medium. The expansion coefficients a_{mn} and b_{mn} are to be determined by matching boundary conditions. Here $\mathbf{M}_{mn}^{(3)}(k_0, \mathbf{r})$ and $\mathbf{N}_{mn}^{(3)}(k_0, \mathbf{r})$ are the outgoing VSWF's [15, 16, 17].

Suppose that the particle is illuminated by a plane wave characterized by the incident wave vector \mathbf{k}_0 , with

$$\mathbf{k}_0 = k_0 (\sin \theta_k \cos \varphi_k \mathbf{e}_x + \sin \theta_k \sin \varphi_k \mathbf{e}_y + \cos \theta_k \mathbf{e}_z), \quad (17)$$

where \mathbf{e}_x , \mathbf{e}_y , and \mathbf{e}_z are three unit base vectors of the Cartesian coordinate system and θ_k (φ_k) is the polar (azimuthal) angle of \mathbf{k}_0 , as schematically shown in Fig.1. The electric and magnetic fields of the incident plane wave are then, for arbitrary polarization mode of incident light,

$$\begin{aligned} \mathbf{E}_{\text{inc}} &= E_0 \hat{\mathbf{p}} e^{i\mathbf{k}_0 \cdot \mathbf{r}} = E_0 (p_\theta \hat{\theta}_k + p_\varphi \hat{\varphi}_k) e^{i\mathbf{k}_0 \cdot \mathbf{r}}, \\ \mathbf{H}_{\text{inc}} &= E_0 \frac{\mathbf{k}_0 \times \hat{\mathbf{p}}}{\omega \mu_0} e^{i\mathbf{k}_0 \cdot \mathbf{r}} = \frac{k_0}{\omega \mu_0} E_0 (p_\theta \hat{\varphi}_k - p_\varphi \hat{\theta}_k) e^{i\mathbf{k}_0 \cdot \mathbf{r}}, \end{aligned} \quad (18)$$

where $\hat{\mathbf{p}} = (p_\theta \hat{\theta}_k + p_\varphi \hat{\varphi}_k)$ is the normalized complex polarization vector, with $|\hat{\mathbf{p}}| = |p_\theta|^2 + |p_\varphi|^2 = 1$, and the unit vectors $\hat{\theta}_k$ and $\hat{\varphi}_k$ are defined in the direction of increasing θ_k and φ_k

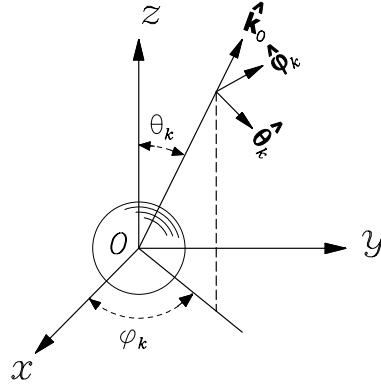


Fig. 1. Geometry of the scattering problem.

such as to constitute a right-hand base system together with $\hat{\mathbf{k}}_0 = \mathbf{k}_0/k_0$, as shown in Fig.1, namely,

$$\hat{\mathbf{k}}_0 \times \hat{\boldsymbol{\theta}}_k = \hat{\boldsymbol{\phi}}_k, \quad \hat{\boldsymbol{\theta}}_k \times \hat{\boldsymbol{\phi}}_k = \hat{\mathbf{k}}_0, \quad \hat{\boldsymbol{\phi}}_k \times \hat{\mathbf{k}}_0 = \hat{\boldsymbol{\theta}}_k. \quad (19)$$

Expanded in terms of VSWF's, the incident fields ($\mathbf{E}_{\text{inc}}, \mathbf{H}_{\text{inc}}$) read

$$\begin{aligned} \mathbf{E}_{\text{inc}} &= - \sum_{n=1}^2 \sum_{m=-n}^n iE_{mn} [p_{mn} \mathbf{N}_{mn}^{(1)}(k_0, \mathbf{r}) + q_{mn} \mathbf{M}_{mn}^{(1)}(k_0, \mathbf{r})] \\ \mathbf{H}_{\text{inc}} &= - \frac{k_0}{\omega \mu_0} \sum_{n=1}^2 \sum_{m=-n}^n E_{mn} [q_{mn} \mathbf{N}_{mn}^{(1)}(k_0, \mathbf{r}) + p_{mn} \mathbf{M}_{mn}^{(1)}(k_0, \mathbf{r})], \end{aligned} \quad (20)$$

where use has been made of $n_c = 2$ for small particle. The expansion coefficients p_{mn} and q_{mn} are

$$\begin{aligned} p_{mn} &= [p_\theta \tau_{mn}(\cos \theta_k) - ip_\phi \pi_{mn}(\cos \theta_k)] e^{-im\phi_k}, \\ q_{mn} &= [p_\theta \pi_{mn}(\cos \theta_k) - ip_\phi \tau_{mn}(\cos \theta_k)] e^{-im\phi_k}, \end{aligned} \quad (21)$$

with the regular angular functions $\pi_{mn}(\cos \theta)$ and $\tau_{mn}(\cos \theta)$ defined based on the first kind associated Legendre functions $P_n^m(\cos \theta)$ [15, 16, 17],

$$\begin{aligned} \pi_{mn}(\cos \theta) &= C_{mn} \frac{m}{\sin \theta} P_n^m(\cos \theta), \\ \tau_{mn}(\cos \theta) &= C_{mn} \frac{d}{d\theta} P_n^m(\cos \theta), \end{aligned} \quad (22)$$

and C_{mn} given in Eq. (6).

Matching the boundary conditions at the surface of sphere and after some algebra, one arrives at the linear set of equations that serve to determine the expansion coefficients α_l , a_{mn} and b_{mn} based on p_{mn} and q_{mn} ,

$$\begin{aligned}
\frac{1}{m_s} \sum_{l=1}^{2n_d} \frac{1}{\bar{k}_l \lambda_l} j_n(\bar{k}_l m_s \eta) w_{mn,l} \alpha_l + \xi'_n(\eta) a_{mn} + \frac{1}{m_s} \sum_{l=1}^{2n_d} \frac{1}{\bar{k}_l} \psi'_n(\bar{k}_l m_s \eta) d_{mn,l} \alpha_l &= \psi'_n(\eta) p_{mn} \\
\xi_n(\eta) b_{mn} + \frac{1}{m_s} \sum_{l=1}^{2n_d} \frac{1}{\bar{k}_l} \psi_n(\bar{k}_l m_s \eta) c_{mn,l} \alpha_l &= \psi_n(\eta) q_{mn} \\
\xi_n(\eta) a_{mn} + \frac{\mu_0}{\mu_s} \sum_{l=1}^{2n_d} \psi_n(\bar{k}_l m_s \eta) d_{mn,l} \alpha_l &= \psi_n(\eta) p_{mn} \\
\xi'_n(\eta) b_{mn} + \frac{\mu_0}{\mu_s} \sum_{l=1}^{2n_d} \psi'_n(\bar{k}_l m_s \eta) c_{mn,l} \alpha_l &= \psi'_n(\eta) q_{mn}
\end{aligned} \tag{23}$$

where

$$\eta = k_0 a, \quad m_s = \frac{\sqrt{1+u_a} k_s}{k_0}, \quad \bar{k}_l = \frac{k_l}{k_s}, \quad \lambda_l = \frac{k_s^2}{k_l^2} = \frac{1}{\bar{k}_l^2}, \tag{24}$$

with a the radius of the scattering spherical particle. The Riccati-Bessel functions $\psi_n(z)$ and $\xi_n(z)$ are given based on the spherical Bessel $j_n(z)$ and spherical Hankel functions $h_n^{(1)}(z)$ by [16]

$$\psi_n(z) = z j_n(z), \quad \xi_n(z) = z h_n^{(1)}(z). \tag{25}$$

The derivative is made with respect to its argument

$$\psi'_n(z) = \frac{d\psi(z)}{dz}, \quad \xi'_n(z) = \frac{d\xi(z)}{dz}.$$

3. Calculation of radiation torque and discussion

With the incident fields and the scattered field given by Eq. (20) and Eq. (16), respectively, the total external field outside the particle read

$$\begin{aligned}
\mathbf{E}_e &= \sum_{n=1}^2 \sum_{m=-n}^n i E_{mn} \left[a_{mn} \mathbf{N}_{mn}^{(3)}(k_0, \mathbf{r}) + b_{mn} \mathbf{M}_{mn}^{(3)}(k_0, \mathbf{r}) - p_{mn} \mathbf{N}_{mn}^{(1)}(k_0, \mathbf{r}) - q_{mn} \mathbf{M}_{mn}^{(1)}(k_0, \mathbf{r}) \right] \\
\mathbf{H}_e &= \frac{k_0}{\omega \mu_0} \sum_{n=1}^2 \sum_{m=-n}^n E_{mn} \left[b_{mn} \mathbf{N}_{mn}^{(3)}(k_0, \mathbf{r}) + a_{mn} \mathbf{M}_{mn}^{(3)}(k_0, \mathbf{r}) - q_{mn} \mathbf{N}_{mn}^{(1)}(k_0, \mathbf{r}) - p_{mn} \mathbf{M}_{mn}^{(1)}(k_0, \mathbf{r}) \right]
\end{aligned} \tag{26}$$

where the expansion coefficients a_{mn} and b_{mn} for the scattered fields are found based on Eq. (23). The time-averaged Maxwell stress tensor is then, for isotropic surrounding medium,

$$\hat{\mathbf{T}} = \frac{1}{2} \text{Re}[\mathbf{E}_e \mathbf{D}_e^* + \mathbf{H}_e \mathbf{B}_e^* - \frac{1}{2} (\mathbf{E}_e \cdot \mathbf{D}_e^* + \mathbf{H}_e \cdot \mathbf{B}_e^*) \hat{\mathbf{I}}] \tag{27}$$

where the superscript $*$ denotes the complex conjugate, and $\hat{\mathbf{I}}$ is the unit dyad. The time-averaged torque $\boldsymbol{\tau}$ on the scatterer can be evaluated by [19, 20]

$$\boldsymbol{\tau} = - \int d\mathbf{S} \cdot \hat{\mathbf{K}} = - \int [\mathbf{e}_r \cdot \hat{\mathbf{K}}] dS \tag{28}$$

where $\mathbf{e}_r = \mathbf{r}/r$ is the unit vector in radial direction with $r = |\mathbf{r}|$, and the time-averaged angular momentum flux tensor $\hat{\mathbf{K}}$ reads [20]

$$\hat{\mathbf{K}} = \hat{\mathbf{T}} \cdot [\mathbf{r} \times \hat{\mathbf{I}}] = \hat{\mathbf{T}} \times \mathbf{r}. \tag{29}$$

As a result, the time-averaged torque becomes

$$\boldsymbol{\tau} = - \int [\mathbf{e}_r \cdot (\hat{\mathbf{T}} \times \mathbf{r})] dS = \int [\mathbf{r} \times (\hat{\mathbf{T}} \cdot \mathbf{e}_r)] dS = r^3 \int \mathbf{e}_r \times [\hat{\mathbf{T}} \cdot \mathbf{e}_r] d\Omega, \quad (30)$$

where the integration $\int \dots d\Omega$ is over the solid angle.

The expression for the radiation torque Eq. (30) should be evaluated at $r = a$, the outer surface of the spherical particle. For lossless background medium, however, with ϵ_0 and μ_0 being both real numbers, the integration Eq. (30) can be performed at spherical surface with arbitrary radius $r > a$, due to conservation of momentum and angular momentum. As a result, the integration is usually evaluated in the limit $r \rightarrow \infty$ for lossless surrounding medium, where the field expressions become much simpler by using the asymptotical formulas for the Riccati-Bessel functions

$$\xi_n(\rho) \sim (-i)^{n+1} \exp(i\rho), \quad \zeta_n(\rho) \sim i^{n+1} \exp(-i\rho), \quad \psi_n(\rho) \sim [\xi_n(\rho) + \zeta_n(\rho)]/2. \quad (31)$$

After lengthy algebra, the expressions for torque can be expressed in terms of the expansion coefficients a_{mn} , b_{mn} , p_{mn} and q_{mn}

$$\tau_x = \text{Re} [\mathcal{N}_1], \quad \tau_y = \text{Im} [\mathcal{N}_1], \quad \tau_z = -\text{Re} [\mathcal{N}_2], \quad (32)$$

where

$$\begin{aligned} \mathcal{N}_1 = & \frac{2\pi\epsilon_0|E_0|^2}{k_0^3} \sum_{n=1}^2 \sum_{m=-n}^{n-1} \rho_{mn} [a_{mn}a_{m_1n}^* + b_{mn}b_{m_1n}^* \\ & - \frac{1}{2}(a_{mn}p_{m_1n}^* + p_{mn}a_{m_1n}^* + b_{mn}q_{m_1n}^* + q_{mn}b_{m_1n}^*)] \end{aligned} \quad (33)$$

$$\begin{aligned} \mathcal{N}_2 = & \frac{2\pi\epsilon_0|E_0|^2}{k_0^3} \sum_{n=1}^2 \sum_{m=-n}^n m [a_{mn}a_{mn}^* + b_{mn}b_{mn}^* \\ & - \frac{1}{2}(a_{mn}p_{mn}^* + p_{mn}a_{mn}^* + b_{mn}q_{mn}^* + q_{mn}b_{mn}^*)] \end{aligned} \quad (34)$$

with $\rho_{mn} = [(n-m)(n+m+1)]^{1/2}$ and $m_1 = m+1$. It is noted that similar expressions were presented by several authors [21, 22, 23, 24].

With Eqs. (32-34), we are now ready to present the analytical results in the small particle limit. To be specific, the EA of the birefringent particle is set as z -axis, without loss of generality. The incident plane is defined by the EA (z -axis) and the incident wave vector \mathbf{k}_0 . The axial symmetry of the permittivity tensor Eq. (2) implies that the scattering is independent of the azimuthal angle φ_k of the incident wave vector \mathbf{k}_0 . For simplicity, we set $\varphi_k = 0$, which means $\hat{\varphi}_k = \mathbf{e}_y$ and \mathbf{k}_0 lies in the x - z plane. The z -component of torque τ_z vanishes due to symmetry, we therefore concentrate on \mathcal{N}_1 , whose real and imaginary parts give τ_x and τ_y , respectively. In addition, as we are interested in the time averaged radiation torque, we assume that p_θ is a non-negative real number while p_φ is a complex number. Obviously, this assumption does not affect the generality for the calculation of the time-averaged torque.

To explore the small particle behavior, the Riccati-Bessel functions and their derivatives in Eq. (23) are all expanded in terms of the size parameter $\eta = k_0a$. Solving Eq. (23) and plugging the results for the expansion coefficients a_{mn} and b_{mn} into Eq. (33), we obtain

$$\mathcal{N}_1 = c_3\eta^3 + c_5\eta^5 + c_6\eta^6 + o(\eta^7), \quad (35)$$

where the coefficients c_3 , c_5 and c_6 are given by

$$\begin{aligned}
c_3 &= \frac{3p_\theta u_a \varepsilon_r [\text{Re} p_\varphi - i p_\theta \cos \theta_k] \sin \theta_k}{4\pi^2 (2 + \varepsilon_r)(u_a \varepsilon_r + \varepsilon_r + 2)} \varepsilon_0 \lambda_0^3 |E_0|^2 \\
c_5 &= [i |p_\varphi|^2 u_a \varepsilon_r (\varepsilon_r - 1)^2 f_0 \sin 2\theta_k + i p_\theta^2 u_a \varepsilon_r (f_1 + f_2 \cos 2\theta_k) \sin 2\theta_k \\
&\quad + u_a \varepsilon_r p_\theta [\text{Re} p_\varphi] (f_3 - f_2 \cos 2\theta_k) \sin \theta_k] \varepsilon_0 \lambda_0^3 |E_0|^2 \\
c_6 &= \frac{3p_\theta u_a^2 \varepsilon_r^2 [\text{Im} p_\varphi] \sin \theta_k}{2\pi^2 (2 + \varepsilon_r)^2 (u_a \varepsilon_r + \varepsilon_r + 2)^2} \varepsilon_0 \lambda_0^3 |E_0|^2
\end{aligned} \tag{36}$$

with $\text{Re} p_\varphi$ and $\text{Im} p_\varphi$ denoting, respectively, the real and imaginary parts of p_φ . f_0 , f_1 , f_2 , f_3 are all real rational functions of u_a and ε_r . Retaining the leading terms, the torque is then given by

$$\tau_x = \frac{6\pi p_\theta [\text{Re} p_\varphi] u_a \varepsilon_r \sin \theta_k}{(2 + \varepsilon_r)(u_a \varepsilon_r + \varepsilon_r + 2)} \varepsilon_0 a^3 |E_0|^2 + \frac{96\pi^4 p_\theta [\text{Im} p_\varphi] u_a^2 \varepsilon_r^2 \sin \theta_k}{(2 + \varepsilon_r)^2 (u_a \varepsilon_r + \varepsilon_r + 2)^2 \lambda_0^3} \varepsilon_0 a^6 |E_0|^2, \tag{37}$$

$$\tau_y = -\frac{3\pi p_\theta^2 u_a \varepsilon_r \sin 2\theta_k}{(2 + \varepsilon_r)(u_a \varepsilon_r + \varepsilon_r + 2)} \varepsilon_0 a^3 |E_0|^2 + \frac{4\pi^3 |p_\varphi|^2 u_a \varepsilon_r (\varepsilon_r - 1)^2 \sin 2\theta_k}{15(2\varepsilon_r + 3)(2\varepsilon_r + 3 + u_a \varepsilon_r) \lambda_0^2} \varepsilon_0 a^5 |E_0|^2, \tag{38}$$

where use has been made of

$$f_0 = \frac{1}{120\pi^2 (2\varepsilon_r + 3)(2\varepsilon_r + 3 + u_a \varepsilon_r)}.$$

It is noted that if one retains only the dominant terms, f_1 , f_2 and f_3 are irrelevant to the explicit analytical expression for the radiation torque, so we do not present their explicit expressions here.

Equations (37) and (38) suggests three different types of a dependence of the radiation torque, depending on the incident direction as well as the incident polarization mode. The most common case is the cubic law dependence $\tau \sim a^3$. This happens for the general elliptically polarized (EP) incident mode, provided that the principal axes of the polarization ellipse do not coincide with $\hat{\theta}_k$ and $\hat{\phi}_k$ axes so that $\text{Re} p_\varphi \neq 0$ and $p_\theta \neq 0$. Here the polarization ellipse denotes the ellipse traced out by the tip of the \mathbf{E}_{inc} vector at a fixed point in space. Retaining only the leading terms in the small particle limit, the torque is given in this general case by

$$\tau_x = \frac{6\pi p_\theta [\text{Re} p_\varphi] u_a \varepsilon_r \sin \theta_k}{(2 + \varepsilon_r)(u_a \varepsilon_r + \varepsilon_r + 2)} \varepsilon_0 a^3 |E_0|^2, \tag{39}$$

$$\tau_y = -\frac{3\pi p_\theta^2 u_a \varepsilon_r \sin 2\theta_k}{(2 + \varepsilon_r)(u_a \varepsilon_r + \varepsilon_r + 2)} \varepsilon_0 a^3 |E_0|^2, \tag{40}$$

which, besides exhibiting a^3 law, is in magnitude approximately proportional to the difference of the electrical susceptibilities in the extraordinary and the ordinary directions $(\chi_e - \chi_o) = u_a \varepsilon_r$. The angle θ_τ between the torque and the major axis of the polarization ellipse is given by

$$\cos \theta_\tau = -\frac{\cos \theta_k}{Q} (p_\theta \sqrt{1 - q} - |\text{Re} p_\varphi| \sqrt{1 + q}) \tag{41}$$

with

$$q = \frac{p_\theta^2 - |p_\varphi|^2}{\{(p_\theta^2 - |p_\varphi|^2)^2 + 4p_\theta^2 [\text{Re} p_\varphi]^2\}^{1/2}} \quad \text{and} \quad Q = \{2p_\theta^2 \cos^2 \theta_k + 2[\text{Re} p_\varphi]^2\}^{1/2}. \tag{42}$$

Apart from the general EP mode, the cubic law dependence of the radiation torque applies also to the general linearly polarized (LP) incidence except the transverse electric (TE) mode that corresponds to the case with the magnetic vector vibrating in the incident plane. In the LP case (except TE), θ_τ given by Eq. (41) determines the angle between the radiation torque and the incident electric field \mathbf{E}_{inc} . With $\text{Re}p_\varphi = p_\varphi$ for the LP incidence, it follows from Eq. (41) that $\cos\theta_\tau = 0$, namely, the radiation torque is perpendicular to \mathbf{E}_{inc} as well as the EA, as proposed in [13]. It can therefore be rewritten in the form

$$\begin{aligned}\boldsymbol{\tau} &= -\frac{6\pi u_a \varepsilon_r p_\theta \sin\theta_k}{(2 + \varepsilon_r)(2 + \varepsilon_r + u_a \varepsilon_r)} \varepsilon_0 a^3 |E_0|^2 \mathbf{e}_z \times (p_\theta \hat{\boldsymbol{\theta}}_k + p_\varphi \hat{\boldsymbol{\phi}}_k) \\ &= \frac{3\pi(\chi_e - \chi_o) \sin 2\phi_e}{(2 + \varepsilon_r)(2 + \varepsilon_r + u_a \varepsilon_r)} \varepsilon_0 a^3 |E_0|^2 \hat{\mathbf{q}}\end{aligned}\quad (43)$$

where $\hat{\mathbf{q}}$ is the unit vector perpendicular to \mathbf{E}_{inc} and the EA, ϕ_e is the angle between \mathbf{E}_{inc} and the EA, given by $\cos\phi_e = -p_\theta \sin\theta_k$ and thus $\pi/2 \leq \phi_e \leq \pi$. Compared with Eq. (1), it is found that

$$\tau_0 = \frac{3\pi}{(2 + \varepsilon_r)(2 + \varepsilon_r + u_a \varepsilon_r)} \varepsilon_0 a^3 |E_0|^2. \quad (44)$$

Physically, the a^3 dependent torque originates from the misalignment, due to the birefringence $\chi_e \neq \chi_o$, between \mathbf{E}_{inc} and the polarization \mathbf{P} induced on the particle.

The second type of power law behavior $\tau \sim a^5$ is found for the TE incident mode, which is excluded in the earlier discussion for the LP cases. For the TE mode, $\tau_x = 0$ by symmetry. Since $p_\theta = 0$, the first term on the right hand side (rhs) of Eq. (38) disappears, and one has

$$\boldsymbol{\tau} = \tau_y \mathbf{e}_y = \frac{4\pi^3 (\varepsilon_r - 1)^2 \varepsilon_r u_a \sin 2\theta_k}{15(2\varepsilon_r + 3)(3 + 2\varepsilon_r + u_a \varepsilon_r) \lambda_0^2} \varepsilon_0 a^5 |E_0|^2 \mathbf{e}_y, \quad (45)$$

where use has been made of $|p_\varphi|^2 = 1 - p_\theta^2 = 1$ for the TE case. The torque is found proportional to $\chi_e - \chi_o$ but parallel to \mathbf{E}_{inc} , presenting a striking contrast to the general LP case with $p_\theta \neq 0$, where $\boldsymbol{\tau}$ is perpendicular to \mathbf{E}_{inc} . The a^5 dependence of the torque is believed to arise physically from the interaction between the external incident field and the radiation field due to the oscillating dipole induced on the particle. Although it is present for most incident modes, it becomes dominant only when the a^3 terms vanish, which occurs when \mathbf{P} coincides with \mathbf{E}_{inc} for TE case.

The third type of a dependence $\tau \sim a^6$ occurs when the particle is subject to normal illumination by the circularly polarized (CP) light or the EP light with the principal axes of the polarization ellipse coinciding with the $\hat{\boldsymbol{\theta}}_k$ and $\hat{\boldsymbol{\phi}}_k$ axes. With $\theta_k = \pi/2$, $\tau_y = 0$ by symmetry. The first term of Eq. (37) vanishes since $\text{Re}p_\varphi = 0$ in the current cases. The torque is then given by

$$\boldsymbol{\tau} = \tau_x \mathbf{e}_x = \frac{96\pi^4 p_\theta \text{Im}(p_\varphi) u_a^2 \varepsilon_r^2 \sin\theta_k}{(2 + \varepsilon_r)^2 (u_a \varepsilon_r + \varepsilon_r + 2)^2 \lambda_0^3} \varepsilon_0 a^6 |E_0|^2 \mathbf{e}_x. \quad (46)$$

In magnitude, the torque is approximately proportional to $(\chi_e - \chi_o)^2 = u_a^2 \varepsilon_r^2$ instead of $(\chi_e - \chi_o)$. It is perpendicular to \mathbf{E}_{inc} as well as the EA.

Take a calcite particle of radius $a = 150$ nm as an example. With the ordinary and extraordinary refractive indices $n_o = 1.658$ and $n_e = 1.486$ [25], and typical incident light of the wave length $\lambda_0 = 1064$ nm and the incident irradiance $I_0 = 10 \times 10^6$ w/cm² [11], the maximum torque based on Eq.(43), Eq.(45), and Eq.(46) will be 5.7×10^2 pN-nm, 9.0 pN-nm, and 2.2×10 pN-nm, respectively.

Now we turn to the rotationally equilibrium orientation of the birefringent particle due to the radiation torque $\boldsymbol{\tau}$. For simplicity, we assume that the birefringent particle is trapped within a viscous fluid medium, as in most practical situations. As a result, in addition to the radiation torque, the particle is also subject to a viscous drag torque proportional to its spinning angular velocity. The orientation subject to vanishing optical torque is therefore regarded as equilibrium. The stability of the equilibrium is analyzed by casting a perturbation and analyzing its reorientation by the radiation torque in the presence of the viscous drag. When the particle is liable to a constant torque, it is said to rotate at a constant velocity due to the presence of the viscous drag.

Let us start with the normal illumination, namely, the case with the incident wave vector \mathbf{k}_0 perpendicular to the EA. With $\theta_k = \pi/2$, we have $\tau_y = 0$ by symmetry and τ_x is given by Eq. (37). If the particle is illuminated by the EP light with the principal axes of the polarization ellipse not coinciding with $\hat{\theta}_k$ and $\hat{\phi}_k$ axes, the first term on the rhs of Eq. (37) dominates since $a/\lambda_0 \ll 1$. For particle with $\chi_e > \chi_o$ ($u_a > 0$), τ_x will have the same sign as $\text{Re}p_\phi$. The torque will therefore align the EA with the major axis of the polarization ellipse. Once the EA becomes parallel to the major axis, the first term on the rhs of Eq. (37) vanishes since $\text{Re}p_\phi = 0$, while the second term will make the EA rotate in the same direction as the rotation of the electric vector, leading to the misalignment between the EA and the major axis, which in turn switches on the non-vanishing first term on the rhs of Eq. (37) and the torque tries to align the EA with the major axis once again. As a result, the EA will finally reach equilibrium at an orientation that is almost parallel to the major axis of the polarization ellipse, where the first and the second terms on the rhs of Eq. (37) balance each other. Similar analysis for particle with $\chi_e < \chi_o$ shows that the EA will reach equilibrium at an orientation nearly normal to the major axis provided that \mathbf{k}_0 is kept perpendicular to the EA. However, when $\chi_e < \chi_o$, any perturbation that makes the EA oblique to the \mathbf{k}_0 will finally cause a reorientation of the EA toward \mathbf{k}_0 , as can be seen below in the discussion for the oblique illumination with $\theta_k \neq \pi/2$. When the polarization ellipse degenerates into a circle, the first term on the rhs of Eq. (37) will always vanish due to $\text{Re}p_\phi = 0$, and the particle is thus always subject to a torque in proportion to a^6 . As a result, a particle with $\chi_e > \chi_o$ will rotate in positive (negative) direction at a constant angular velocity about the \mathbf{k}_0 -axis for left (right) CP incidence. For a particle with $\chi_e < \chi_o$, such kind of rotation is not stable against perturbation. Its EA will be made parallel to the \mathbf{k}_0 eventually. When the polarization ellipse degenerates into a straight line, the EA of the particle with $\chi_e > \chi_o$ ($\chi_e < \chi_o$) is aligned with \mathbf{E}_{inc} (\mathbf{H}_{inc}) and reaches a stable equilibrium.

Next we turn to the oblique illumination with $\theta_k \neq \pi/2$. When the incident wave is EP or CP, $p_\theta \neq 0$ and thus τ_y is given by Eq. (40). For a particle with $\chi_e > \chi_o$, τ_y is negative (positive) for $0 < \theta_k < \pi/2$ ($\pi/2 < \theta_k < \pi$), implying that the radiation torque tends to make the EA of the particle parallel to the plane of the incident electric field \mathbf{E}_{inc} (namely, the plane normal to \mathbf{k}_0). The presence of τ_x only affects the transient time needed for the EA to become parallel to this plane. Once the EA lies in the plane of \mathbf{E}_{inc} , the analysis for the case of normal illumination applies. As a result, the EA will finally be aligned with the direction that is almost parallel to the major axis of the polarization ellipse for the EP incidence, or it will rotate in positive (negative) direction about the \mathbf{k}_0 -axis for the left (right) CP mode. For particle with $\chi_e < \chi_o$, on the other hand, τ_y given by Eq. (40) is always positive (negative) for $0 < \theta_k < \pi/2$ ($\pi/2 < \theta_k < \pi$), indicating that the EA will be finally aligned with the \mathbf{k}_0 by the EP or CP light. The most experimentally relevant may be the cases in which the polarization ellipse degenerates into a straight line. For general case with $p_\theta \neq 0$, the radiation torque is perpendicular to \mathbf{E}_{inc} as well as the EA. Noticing that the EA is set as the z -axis and \mathbf{E}_{inc} is parallel to $p_\theta \hat{\theta}_k + p_\phi \hat{\phi}_k$, it follows

from Eq. (43) that

$$t_E \equiv \frac{(\mathbf{e}_z \times \mathbf{E}_{\text{inc}}) \cdot \boldsymbol{\tau}}{\mathbf{e}_z \cdot \mathbf{E}_{\text{inc}}} = \frac{6\pi\epsilon_r u_a (p_\phi^2 + p_\theta^2 \cos^2 \theta_k)}{(2 + \epsilon_r)(2 + \epsilon_r + u_a \epsilon_r)} \epsilon_0 a^3 |E_0|^2. \quad (47)$$

For a particle with $\chi_e > \chi_o$, because $t_E > 0$, its EA will be aligned with \mathbf{E}_{inc} by the radiation torque. For a particle with $\chi_e < \chi_o$, since $t_E < 0$, the radiation torque inclines to switch the EA parallel to the \mathbf{k}_0 - \mathbf{H}_{inc} plane, namely, the plane normal to \mathbf{E}_{inc} . Once the EA lies in the \mathbf{k}_0 - \mathbf{H}_{inc} plane, the particle is left with the TE incident mode, its EA will further be aligned with \mathbf{H}_{inc} as discussed below. For the TE incident mode with $p_\theta = 0$, the radiation torque, given by Eq. (45), is parallel to the electric field and in proportion to a^5 . The torque will align the EA with \mathbf{k}_0 (\mathbf{H}_{inc}) for particle with $\chi_e > \chi_o$ ($\chi_e < \chi_o$) if the EA is kept normal to \mathbf{E}_{inc} . However, for particle with $\chi_e > \chi_o$, any perturbation that makes the EA oblique to \mathbf{E}_{inc} will introduce a non-vanishing p_θ , turning on the a^3 term on the rhs of Eq. (38), which results in a reorientation of the EA toward \mathbf{E}_{inc} eventually. Only for particle with $\chi_e < \chi_o$, can the EA be kept in the plane of polarization (i.e., the \mathbf{k}_0 - \mathbf{H}_{inc} plane) and finally be switched to \mathbf{H}_{inc} by the torque proportional to a^5 .

In Table 1, we summarize the final orientation of the EA due to the radiation torque in the presence of viscous drag. The first row denotes the polarization mode of the incident light. The second and third rows are the final EA orientation for particle with $\chi_e > \chi_o$ and $\chi_e < \chi_o$, respectively.

Table 1. Final orientation of the extraordinary axis by the radiation torque

	elliptical polarization	circular polarization	linear polarization
$\chi_e > \chi_o$	normal to \mathbf{k}_0 and nearly parallel to the major axis of the polarization ellipse	normal to \mathbf{k}_0 and rotating about the \mathbf{k}_0 -axis	parallel to \mathbf{E}_{inc}
$\chi_e < \chi_o$	parallel to \mathbf{k}_0	parallel to \mathbf{k}_0	parallel to \mathbf{H}_{inc}

4. Summary

We have presented an analytical calculation of the radiation torque on a spherical birefringent particle illuminated by plane electromagnetic wave of arbitrary polarization mode and direction of propagation in the small particle limit. The calculation is based on the extended Mie theory and the Maxwell stress tensor formalism. It is found that the radiation torque τ versus the particle radius a may display different power law behaviors, $\tau \sim a^\gamma$, with the exponent $\gamma = 3, 5,$ and 6 , depending on the orientation of the birefringent particle as well as the polarization mode of the incident plane wave. For different incident polarization modes, the radiation torque may be normal or parallel to the incident electric field \mathbf{E}_{inc} , its magnitude may be proportional to $(\chi_o - \chi_e)$ or $(\chi_o - \chi_e)^2$. In the presence of viscous drag, the EA of the birefringent particle can be eventually aligned with \mathbf{E}_{inc} , \mathbf{H}_{inc} , \mathbf{k}_0 , or even kept rotating about the \mathbf{k}_0 -axis at a constant angular velocity, depending on the incident polarization mode and material birefringence of the particle, as summarized in Table 1.

Our analytical calculation is believed relevant to many applications where birefringent spherical particles are implemented, typical in the case of making measurement of viscosity on a microscopic scale [9]. We note that in reality most experiments available on optical torque are

performed using laser beam, and the particles are not so small compared with the incident wave length. We therefore make no direct comparison with the experimental results. However, our explicit analytical expression for the radiation torque provides a limiting case against which the solution of more complicated problems can be checked. In addition, the analysis may be expected to find applications in controlling the orientation of birefringent nanoparticle by laser beams, since the radiation torque can be up to over 500 pN-nm for a particle of radius 150 nm under the illumination of moderate incident irradiance. Numerical calculation is in progress for the torque on larger birefringent particle illuminated by focused laser beam, which is expected to be directly comparable with the currently available experimental results.

Acknowledgments

The work is supported by CNKBRSE, NSFC through 10474014 and 10321003, and PCSIRT.